

Ferroelectric phenomena in CdSnO₃: a first-principles study

A. I. Lebedev*

Physics Department, Moscow State University, Moscow, 119991 Russia

(Dated: January 8, 2016)

The phonon spectrum of cubic cadmium metastannate and the crystal structures of its distorted phases were calculated from first principles within the density functional theory. It is shown that the phonon spectrum and the energy spectrum of distorted phases in α -CdSnO₃ are surprisingly similar to the corresponding spectra of CdTiO₃. The ground state of α -CdSnO₃ is the ferroelectric $Pbn2_1$ phase; the energy gain accompanying the phase transition from the nonpolar $Pbmm$ phase to this phase is ~ 30 meV and the spontaneous polarization in it is 0.25 C/m². An analysis of the eigenvector of the ferroelectric mode in α -CdSnO₃ and calculations of the partial densities of states indicates that the ferroelectric instability in this crystal, which does not contain d transition elements, is associated with the formation of a covalent bonding between Cd and O atoms.

DOI: 10.1134/S1063783409090182

PACS numbers: 61.50.Ah, 63.20.D-, 77.84.Dy

I. INTRODUCTION

In a large family of ferroelectrics with the ABO_3 perovskite structure, crystals in which A is the cadmium atom are least studied. In the CdO–SnO₂ system there are two compounds, CdSnO₃ and Cd₂SnO₄.¹ Cadmium metastannate CdSnO₃ exists in two stable modifications: one with an orthorhombically distorted perovskite structure (α -modification)^{1–3} and the other with the rhombohedral ilmenite structure (β -modification).^{3,4} Like cadmium titanate, CdSnO₃ samples with the ilmenite structure can be synthesized at temperatures $\leq 800^\circ\text{C}$ ^{5,6} and the samples with the perovskite structure at $1000\text{--}1100^\circ\text{C}$ ^{1,5} or at high pressures.³ In addition, CdSnO₃ samples with a metastable spinel structure can be obtained upon decomposition of CdSn(OH)₆.⁷ Cadmium orthostannate Cd₂SnO₄ also exists in two crystal modifications: one with the orthorhombic Sr₂PbO₄ structure and the other with the spinel structure.⁷ All these compounds are n -type semiconductors with a band gap of 2–3 eV.^{8,9} Because of a high concentration of native defects, they are characterized by a rather high conductivity ($\sigma = 10^{-5}\text{--}5 \times 10^3 \Omega^{-1}\text{cm}^{-1}$). This conductivity prevents the study of these materials by dielectric methods. Cadmium stannates are used for fabrication of conducting thin-film coatings transparent to visible light (as transparent conductive oxides) and as gas sensors.

Cadmium metastannate with the perovskite structure is of interest as a potential ferroelectric. Unfortunately, there have been only a few studies of this material. The crystal structure of α -CdSnO₃ was studied at 300 K on powders¹ and single crystals³ and was identified as a structure with the $Pbnm$ space group. A refined analysis of X-ray reflection intensities¹⁰ suggested the possibility of a polar character of this structure (the proposed space group is $Pbn2_1$). The same conclusion was made in Ref. 11. An analysis of the optical absorption and luminescence spectra⁹ revealed, in the temperature dependence of the band gap $E_g(T)$ for α -CdSnO₃ single crystals of unknown orientation, a rapid change in E_g (by

0.11 eV) at $T \approx 80^\circ\text{C}$ and two more regions of change near 140 and 200°C , which were associated with phase transitions. In this temperature range, drastic changes in the luminescence intensity and degree of its polarization were also observed. If these peculiarities are really due to the ferroelectric phase transition, we deal with a rare case when the ferroelectric properties appear in perovskite crystals, which do not contain d transition elements.

The objective difficulties of studying cadmium metastannate, incompleteness of the experimental data in the literature, and the lack of understanding of the nature of ferroelectricity proposed in this compound make it desirable to calculate the physical properties of α -CdSnO₃ from first principles.

II. CALCULATION TECHNIQUE

The calculations were performed within the density functional theory using the pseudopotentials and plane wave expansion of wave functions as implemented in the ABINIT code.¹² The exchange-correlation interaction was described in the local density approximation (LDA) following Ref. 13. The pseudopotentials used were optimized separable nonlocal pseudopotentials¹⁴ constructed using the OPIUM program; the local potential correction¹⁵ was added to them to improve their transferability. The parameters used for constructing the pseudopotentials, the results of their testing, and other details of calculations are given in Ref. 16.

III. RESULTS

A. Comparison of the properties of CdSnO₃ and CdTiO₃

Fig. 1 shows the phonon spectra of α -CdSnO₃ and CdTiO₃ crystals in the cubic parent phase with the per-

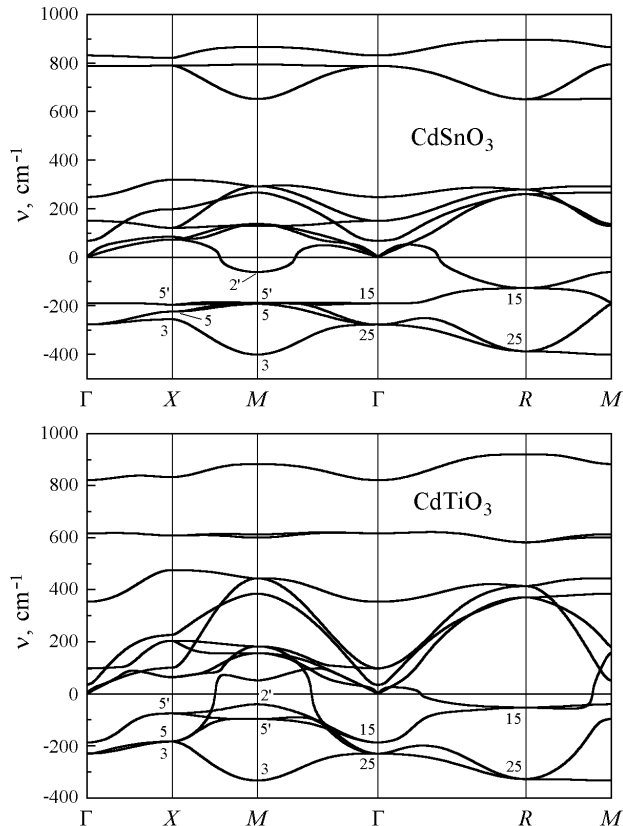


FIG. 1. Comparison of the phonon spectrum for the cubic parent phase of CdSnO_3 with the phonon spectrum of the same phase of CdTiO_3 (Ref. 16). Labels near the curves indicate the symmetry of the modes.

ovskite structure. The comparison of these spectra reveals their surprising similarity. This enables one to suppose that other physical properties of these crystals are also similar.

The energies of different low-symmetry phases formed upon distortion of the cubic parent phase of CdSnO_3 according to the eigenvectors of unstable phonons found in its phonon spectrum are given in Table I. For comparison, the results of previous calculations of the energies of distorted phases in cadmium titanate^{16,17} are included in the table. The existence of one more unstable M_5 mode in CdSnO_3 , which describes the octahedral rotations in the structure, results in two more low-symmetry phases with $Cmma$ and $Pmna$ space groups. It is evident that the energy spectra of different distorted phases in $\alpha\text{-CdSnO}_3$ and CdTiO_3 are very similar, which confirms the similarity of these crystals. The nonpolar phase with the lowest energy in cadmium metastannate is the orthorhombic $Pbnm$ phase.

Table II presents the calculated structural parameters for the $Pbnm$ phase of cadmium metastannate. As follows from the comparison with the literature data, the calculated lattice parameters are close to the experimen-

tally observed ones. A slight overestimate of the calculated lattice parameters is associated with the peculiarity of the Sn pseudopotential, which manifests itself in tests as overestimated lattice parameters of SnO_2 and gray tin. The atomic coordinates in the unit cell agree well with the results of the structure determination of $\alpha\text{-CdSnO}_3$,¹⁸ which was performed under the assumption that the space group of the crystal is $Pbnm$.

Simultaneously with calculating the structure of $\alpha\text{-CdSnO}_3$, the structure of $\beta\text{-CdSnO}_3$ (space group $R\bar{3}$) was obtained. The calculated lattice parameters of this phase ($a = 5.5238 \text{ \AA}$, $c = 14.6550 \text{ \AA}$) were found to be close to those obtained experimentally ($a = 5.4530 \text{ \AA}$, $c = 14.960 \text{ \AA}$, Ref. 3). The energy of the $R\bar{3}$ phase of cadmium metastannate was by 77 meV lower than that of the $Pbn2_1$ phase. This means that at $T = 0$ the phase with the distorted perovskite structure is metastable. It should be noted that according to our data, in CdTiO_3 , which also exists in ilmenite and perovskite modifications, the energy of the $R\bar{3}$ phase at $T = 0$ is by 166 meV lower than that of the $Pbnm$ phase. The difference in the entropy contributions to the thermodynamic potential Φ can result in intersection of the curves for $\Phi(T)$ for the two considered phases. This can explain why one obtains crystals with the ilmenite structure at a low synthesis temperature and crystals with the perovskite structure at a high synthesis temperature (see Sec. I).

B. Ferroelectric phase in CdSnO_3

In order to check the possibility of ferroelectricity in $\alpha\text{-CdSnO}_3$, the frequencies of phonons at the Γ point were calculated for the orthorhombic $Pbnm$ phase of this crystal. The calculations revealed one unstable B_{1u} mode with a frequency of $89i \text{ cm}^{-1}$, which can be associated with the ferroelectric phase transition $Pbnm \rightarrow Pbn2_1$.

The calculated equilibrium atomic positions and lattice parameters for the $Pbn2_1$ phase are given in Table II. The lattice distortion is accompanied by a noticeable rearrangement of the local environment of the Cd atom; it results in that the average distance to four nearest oxygen atoms increases by 0.017 \AA but another two oxygen atoms become closer by 0.23 \AA . Thus, the ferroelectric lattice distortion is accompanied by an increase in the effective coordination number of the Cd atom. The energy gain from the $Pbnm \rightarrow Pbn2_1$ phase transition is $\Delta E = 30.5 \text{ meV}$ (Table I). The sufficiently high energy gain enables one to expect that the structure will be ferroelectric at room temperature, in agreement with the data of Refs. 10 and 11. Indeed, the phase transition temperature ($\Delta E/k \sim 350 \text{ K}$) estimated from the energy gain upon the transition to the ferroelectric phase is close to the temperature of 80°C , at which the most drastic changes in the absorption spectra were observed.⁹ The calculation of the spontaneous polarization in CdSnO_3 with $Pbn2_1$ structure using the Berry phase method¹⁹ gives an unexpectedly high value of $P_s = 0.25 \text{ C/m}^2$,

TABLE I. Comparison of the relative energies of different low-symmetry phases of CdTiO₃ and CdSnO₃. The energy of the cubic phase was taken as the energy origin. The energies of the ground states are in boldface.

| CdTiO ₃ ^a | | | CdSnO ₃ | | |
|--|---------------------------|--------------|--|---------------------------|--------------|
| Unstable mode | Space group | Energy (meV) | Unstable mode | Space group | Energy (meV) |
| <i>R</i> ₁₅ | <i>I4/mmm</i> | -24 | <i>M</i> ₅ | <i>Cmma</i> | -141 |
| <i>X</i> ₃ | <i>P4₂/mmc</i> | -45 | <i>M</i> ₅ | <i>Pmna</i> | -262 |
| Γ ₂₅ | <i>P4̄m2</i> | -134 | <i>X</i> ₃ | <i>P4₂/mmc</i> | -404 |
| <i>X</i> ₅ | <i>Pmma</i> | -160 | <i>X</i> ₅ | <i>Pmma</i> | -474 |
| Γ ₁₅ | <i>R3m</i> | -245 | <i>R</i> ₁₅ | <i>I4/mmm</i> | -536 |
| <i>X</i> ₅ | <i>Cmcm</i> | -282 | Γ ₂₅ | <i>P4̄m2</i> | -540 |
| Γ ₁₅ | <i>P4mm</i> | -340 | Γ ₁₅ | <i>R3m</i> | -753 |
| Γ ₁₅ , Γ ₂₅ | <i>Amm2</i> | -412 | <i>X</i> ₅ | <i>Cmcm</i> | -886 |
| Γ ₂₅ | <i>R32</i> | -486 | Γ ₁₅ | <i>P4mm</i> | -1079 |
| <i>R</i> ₂₅ | <i>I4/mcm</i> | -912 | Γ ₁₅ , Γ ₂₅ | <i>Amm2</i> | -1259 |
| <i>M</i> ₃ | <i>P4/mbm</i> | -920 | Γ ₂₅ | <i>R32</i> | -1450 |
| <i>R</i> ₂₅ | <i>R3̄c</i> | -1197 | <i>M</i> ₃ | <i>P4/mbm</i> | -1617 |
| <i>R</i> ₁₅ | <i>C2/m</i> | -1202 | <i>R</i> ₂₅ | <i>I4/mcm</i> | -1659 |
| <i>R</i> ₂₅ + <i>M</i> ₃ | <i>Pbnm</i> | -1283 | <i>R</i> ₁₅ | <i>C2/m</i> | -2455 |
| <i>B</i> _{2u} | <i>Pb2₁m</i> | -1285 | <i>R</i> ₂₅ | <i>R3̄c</i> | -2460 |
| <i>B</i> _{1u} | <i>Pbn2₁</i> | -1290 | <i>R</i> ₂₅ + <i>M</i> ₃ | <i>Pbnm</i> | -2575 |
| | | | <i>B</i> _{1u} | <i>Pbn2₁</i> | -2605 |

^aReferences 16 and 17.

TABLE II. Lattice parameters *a*, *b*, and *c* (in Å) and atomic coordinates in CdSnO₃ crystals with *Pbnm* and *Pbn2₁* space groups.

| Parameter | This work | | Experiment | | | |
|--|-------------|-------------------------|------------|--------|---------|----------------------|
| | <i>Pbnm</i> | <i>Pbn2₁</i> | Ref. 1 | Ref. 3 | Ref. 11 | Ref. 18 ^a |
| <i>a</i> | 5.5024 | 5.5284 | 5.547 | 5.4578 | 5.4593 | 5.4588 |
| <i>b</i> | 5.5982 | 5.5972 | 5.577 | 5.5773 | 5.5804 | 5.5752 |
| <i>c</i> | 7.9770 | 7.9584 | 7.867 | 7.8741 | 7.8771 | 7.8711 |
| Cd _{<i>x</i>} | -0.00861 | -0.00553 | | | | -0.0092 |
| Cd _{<i>y</i>} | +0.04816 | +0.03818 | | | | +0.0423 |
| Cd _{<i>z</i>} | +0.25000 | +0.26021 | | | | +0.2500 |
| Sn _{<i>x</i>} | +0.00000 | +0.00036 | | | | +0.0000 |
| Sn _{<i>y</i>} | +0.50000 | +0.51455 | | | | +0.5000 |
| Sn _{<i>z</i>} | +0.00000 | -0.00209 | | | | +0.0000 |
| O1 _{<i>x</i>} | +0.12498 | +0.12340 | | | | +0.114 |
| O1 _{<i>y</i>} | +0.42809 | +0.42802 | | | | +0.455 |
| O1 _{<i>z</i>} | +0.25000 | +0.24122 | | | | +0.250 |
| O2 _{<i>a</i>} _{<i>x</i>} | +0.68331 | +0.66193 | | | | +0.695 |
| O2 _{<i>a</i>} _{<i>y</i>} | +0.31304 | +0.35381 | | | | +0.301 |
| O2 _{<i>a</i>} _{<i>z</i>} | +0.06830 | +0.04275 | | | | +0.058 |
| O2 _{<i>b</i>} _{<i>x</i>} | +0.31669 | +0.29516 | | | | +0.305 |
| O2 _{<i>b</i>} _{<i>y</i>} | +0.68696 | +0.72657 | | | | +0.699 |
| O2 _{<i>b</i>} _{<i>z</i>} | -0.06830 | -0.09020 | | | | -0.058 |

^aIn the structure determination, the space group was assumed to be *Pbnm*.

which is close to spontaneous polarization in barium titanate.

IV. DISCUSSION

The results of our calculations show that the ferroelectricity can appear in perovskites that do not contain atoms of d transition elements. Let us try to understand the nature of such phase transitions.

The appearance of the ferroelectric phase transition in α -CdSnO₃ cannot be associated with an off-centering of cadmium atoms. Although in the cubic parent phase of CdSnO₃ the diagonal element of the on-site force constant matrix for Cd atoms is -0.0111 Ha/Bohr², which indicates its off-center position, in the $Pbnm$ phase, after the unit cell volume was decreased by 8.4%, the minimum value of the diagonal element increases to $+0.0714$ Ha/Bohr², and the potential well for the Cd atom becomes on-center.²⁰

Now, we consider the characteristics of the ferroelectric soft mode. The eigenvectors ξ of the dynamic matrix for the B_{1u} mode in α -CdSnO₃ and CdTiO₃ and, for comparison, of the Γ_{15} mode in BaTiO₃ are given in Table III. Here, O1 denotes the oxygen atoms which form, along with the B atoms, the chains which propagate along the polar axis of the ferroelectric phase, and O2 denotes the other oxygen atoms. An analysis of the eigenvector of the B_{1u} mode in α -CdSnO₃ shows that the main contribution to this ferroelectric mode is made by Cd and O2 atoms. The Sn atoms exhibit substantial displacements only in the y direction perpendicular to the polar axis and their small displacements along the polar axis are out-of-phase with the Cd atoms and in-phase with the oxygen atoms. This means that cadmium atoms play the main role in the appearance of ferroelectricity in α -CdSnO₃. From the comparison of the eigenvectors of ferroelectric modes in the above three crystals it follows that CdSnO₃ and BaTiO₃ can be considered as limiting cases in which the appearance of ferroelectricity is caused by A and B atoms in the ABO_3 perovskite structure, whereas cadmium titanate can be regarded as an intermediate case.

The Born effective charges Z^* of atoms in the $Pbnm$ phase of cadmium metastannate (Table III) are close to nominal charges of constituent ions. In the cubic parent phase, the effective charge of Sn atoms is slightly smaller than that in the orthorhombic phase ($Z^* = 4.17$) and, for Cd atoms, it is slightly larger ($Z^* = 3.26$).

For better understanding of the nature of ferroelectric instability and of the character of chemical bonding in α -CdSnO₃, the partial densities of states (contributions of s , p , and d orbitals of Cd, Sn, O1, and O2 atoms to the total density of states) were calculated. The results of these calculations are presented in Fig. 2. As follows from the figure, the overlap of Cd $4d$ states and O $2p$ states plays an important role in the formation of chemical bonding in the crystal; comparable contributions from

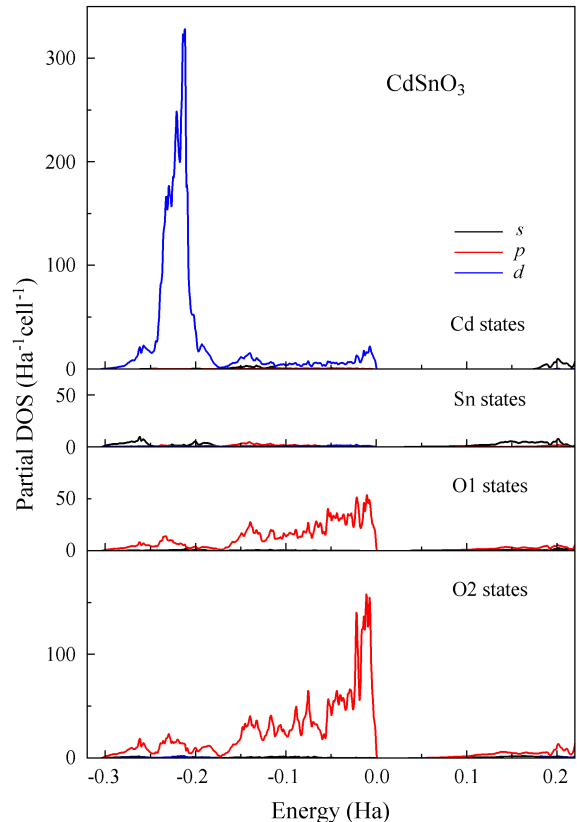


FIG. 2. (Color online) Partial contributions of the s , p , and d states of Cd, Sn, O1, and O2 atoms to the density of states in the $Pbnm$ phase of CdSnO₃. The energy origin is taken at the top of the valence band.

these states give evidence for a noticeable covalent component in this bonding. The contribution of Sn $5s$ and Sn $5p$ states to the valence band is much smaller than that of Cd atoms, which suggests a predominantly ionic character of the Sn–O bond. The Sn $5s$ states overlapping with O $2p$ states make the main contribution to the conduction band ($E > 0.037$ Ha in Fig. 2). It should be noted that, although the partial densities of states for α -CdSnO₃ have been already calculated in Ref. 18, the role of Cd $4d$ states, whose contribution to the density of states is several times greater than the contribution of Sn $5s$ states according to our data, was not analyzed in that paper. The conclusion about the important role of covalent interaction between Cd and O atoms, which follows from the analysis of partial densities of states, agrees with the results of the analysis of the eigenvector of the ferroelectric mode and suggests that the rearrangement of these bonds is the cause of the ferroelectric instability in α -CdSnO₃.

Table IV presents the calculated frequencies of modes active in Raman and infrared (IR) spectra for CdSnO₃ crystals with $Pbnm$ and $Pbn2_1$ space groups. In a crystal with the $Pbnm$ structure, there are 24 Raman active

TABLE III. Eigenvectors ξ of the ferroelectric B_{1u} mode and effective charges Z^* of atoms in CdSnO_3 and CdTiO_3 crystals with $Pbnm$ space group and in BaTiO_3 with $Pm3m$ space group.

| Atom | ξ_x | ξ_y | ξ_z | Z_{xx}^* | Z_{yy}^* | Z_{zz}^* |
|------|----------|----------|----------|------------|------------|------------|
| Cd | +0.00000 | +0.00000 | +0.18913 | +2.462 | +2.506 | +2.440 |
| Sn | +0.00257 | +0.12515 | -0.01935 | +4.379 | +4.407 | +4.338 |
| O1 | +0.00000 | +0.00000 | -0.05940 | -2.052 | -1.894 | -2.905 |
| O2 | -0.13111 | +0.20564 | -0.19455 | -2.395 | -2.509 | -1.937 |
| Cd | +0.00000 | +0.00000 | +0.10628 | +2.570 | +2.500 | +2.592 |
| Ti | +0.01863 | -0.19067 | +0.15463 | +7.363 | +7.693 | +7.260 |
| O1 | +0.00000 | +0.00000 | -0.16286 | -2.194 | -1.957 | -5.650 |
| O2 | -0.07161 | +0.18255 | -0.19322 | -3.869 | -4.118 | -2.101 |
| Ba | | | +0.02988 | | | +2.738 |
| Ti | | | +0.67340 | | | +7.761 |
| O1 | | | -0.54043 | | | -6.128 |
| O2 | | | -0.35607 | | | -2.186 |

TABLE IV. Calculated frequencies ν_i of the IR and Raman active modes for CdSnO_3 crystals with $Pbnm$ and $Pbn2_1$ space groups.

| Space group | Mode | ν_i (cm^{-1}) |
|-------------|----------|--|
| $Pbnm$ | A_g | 79, 130, 196, 290, 413, 452, 522 |
| | B_{1g} | 108, 150, 232, 347, 440, 500, 671 |
| | B_{2g} | 87, 207, 446, 474, 668 |
| | B_{3g} | 107, 142, 375, 500, 590 |
| | B_{1u} | 89i, 118, 163, 237, 390, 551, 594 |
| | B_{2u} | 62, 150, 175, 226, 264, 302, 420, 512, 605 |
| | B_{3u} | 90, 131, 186, 216, 267, 362, 420, 476, 640 |
| $Pbn2_1$ | A_1 | 78, 117, 138, 144, 201, 213, 241, 271, 375, 413, 436, 504, 562, 574 |
| | A_2 | 93, 105, 121, 130, 149, 202, 226, 263, 351, 396, 432, 486, 539, 599, 655 |
| | B_1 | 90, 120, 152, 206, 236, 251, 273, 351, 396, 443, 466, 483, 610, 658 |
| | B_2 | 88, 131, 151, 193, 208, 238, 261, 298, 364, 421, 462, 515, 579, 603 |

modes (modes with A_g , B_{1g} , B_{2g} , and B_{3g} symmetries) and 25 IR active modes (modes with B_{1u} , B_{2u} , and B_{3u} symmetries). When the symmetry of a crystal is lowered to $Pbn2_1$, all 57 optical modes become active in the Raman spectra and 42 modes of A_1 , B_1 , and B_2 symmetry become active in the IR spectra. Unfortunately, the IR absorption spectra for $\alpha\text{-CdSnO}_3$ obtained in the 250–800 cm^{-1} range in Ref. 21 consist of five very wide bands, and their identification was not possible.

As for the prospects of further studies of ferroelectric properties of $\alpha\text{-CdSnO}_3$, we should note the following. As was noted in Sec. I, these crystals are n -type semiconductors and their temperature dependence of conductiv-

ity follows the Arrhenius law with an activation energy of 0.3 eV.³ Therefore, if the hopping conductivity is not high, studies of them at low temperatures are possible. Donor levels supplying electrons to the conduction band are usually attributed to the oxygen vacancies. However, a rather small effect of variations in O_2 partial pressure on the conductivity of $\alpha\text{-CdSnO}_3$ in the annealing experiments⁸ makes this explanation unlikely. In Ref. 22, in discussing the properties of Cd_2SnO_4 , the energy positions of various defects were calculated and it was shown that the Cd_{Sn} antisite defect is the most important defect in this crystal. Perhaps, the same defects are responsible for the electrical conductivity of $\alpha\text{-CdSnO}_3$. We hope that improvements in the technology of the crystal growth and doping of them with acceptors will make it possible in the future to obtain high-resistivity crystals of $\alpha\text{-CdSnO}_3$, which will enable one to perform direct dielectric measurements.

V. CONCLUSIONS

The first-principles calculations confirm the existence of a stable ferroelectric $Pbn2_1$ phase in cadmium metatannate, whose energy is by 30.5 meV lower than that of the nonpolar $Pbnm$ phase and whose spontaneous polarization is 0.25 C/m². An analysis of the eigenvector of the ferroelectric mode and calculations of the partial densities of states show that the ferroelectric instability in $\alpha\text{-CdSnO}_3$, which does not contain d transition elements, is associated with the formation of the covalent bonding between Cd and O atoms.

ACKNOWLEDGMENTS

This work was supported by the Russian Foundation for Basic Research (project no. 08-02-01436).

-
- * swan@scon155.phys.msu.ru
- ¹ A. J. Smith, *Acta Cryst.* **13**, 749 (1960).
 - ² I. Naray-Szabo, *Naturwissenschaften* **31**, 202 (1943).
 - ³ R. D. Shannon, J. L. Gillson, and R. J. Bouchard, *J. Phys. Chem. Solids* **38**, 877 (1977).
 - ⁴ I. Morgenstern-Badarau, P. Poix, and A. Michel, *Comptes Rendue Acad. Sci. (Paris)* **258**, 3036 (1964).
 - ⁵ Z. Tianshu, S. Yusheng, D. Wang, and F. Huajun, *J. Mater. Sci. Lett.* **13**, 1647 (1994).
 - ⁶ Y.-L. Liu, Y. Xing, H.-F. Yang, Z.-M. Liu, Y. Yang, G.-L. Shen, and R.-Q. Yu, *Anal. Chim. Acta* **527**, 21 (2004).
 - ⁷ *Landolt-Bornstein. Numerical data and functional relationships in science and technology. New Series. Group III.*, Vol. 7d1g (Springer-Verlag, 1986).
 - ⁸ F. Golestani-Fard, C. A. Hogarth, and D. N. Waters, *J. Mater. Sci. Lett.* **2**, 505 (1983).
 - ⁹ E. N. Myasnikov, R. I. Spinko, E. A. Shalaeva, and T. P. Myasnikova, *Ferroelectrics* **214**, 177 (1998).
 - ¹⁰ V. N. Lebedev, R. V. Kolesova, and E. G. Fesenko, in *Crystallization and Properties of Crystals*, Vol. 4 (Novocherkassk Polytechnical Institute, 1977) p. 96.
 - ¹¹ N. V. Prutsakova and Y. V. Kabirov, in *Investigated in Russia (Electronic Journal)*, Vol. 7 (2004) pp. 2402–2409.
 - ¹² X. Gonze, J.-M. Beuken, R. Caracas, F. Detraux, M. Fuchs, G.-M. Rignanese, L. Sindic, M. Verstraete, G. Zerah, F. Jollet, M. Torrent, A. Roy, M. Mikami, P. Ghosez, J.-Y. Raty, and D. C. Allan, *Comput. Mater. Sci.* **25**, 478 (2002).
 - ¹³ J. P. Perdew and A. Zunger, *Phys. Rev. B* **23**, 5048 (1981).
 - ¹⁴ A. M. Rappe, K. M. Rabe, E. Kaxiras, and J. D. Joannopoulos, *Phys. Rev. B* **41**, 1227 (1990).
 - ¹⁵ N. J. Ramer and A. M. Rappe, *Phys. Rev. B* **59**, 12471 (1999).
 - ¹⁶ A. I. Lebedev, *Phys. Solid State* **51**, 362 (2009).
 - ¹⁷ A. I. Lebedev, *Phys. Solid State* **51**, 802 (2009).
 - ¹⁸ H. Mizoguchi, H. W. Eng, and P. M. Woodward, *Inorg. Chem.* **43**, 1667 (2004).
 - ¹⁹ N. Sai, K. M. Rabe, and D. Vanderbilt, *Phys. Rev. B* **66**, 104108 (2002).
 - ²⁰ In this work, the values of the force constants and the partial densities of states are given in Hartree atomic units.
 - ²¹ I. L. Botto and E. J. Baran, *Z. Anorg. Allg. Chem.* **465**, 186 (1980).
 - ²² S. B. Zhang and S.-H. Wei, *Appl. Phys. Lett.* **80**, 1376 (2002).